

# Geophysical Research Letters<sup>®</sup>



## RESEARCH LETTER

10.1029/2022GL099369

### Key Points:

- We observe a similar moment-volume scaling for volcano seismicity, contrasting with the range exhibited by injection-induced examples
- The results show that scaling between moment release and volume change can be used to estimate intruded volumes
- This also provides insights into the geologic factors which control the crust's response to volume changes

### Supporting Information:

Supporting Information may be found in the online version of this article.

### Correspondence to:

T. Kettlety,  
[tom.kettlety@earth.ox.ac.uk](mailto:tom.kettlety@earth.ox.ac.uk)

### Citation:

Kettlety, T., Kendall, J. M., & Roman, D. C. (2022). Self-similarity of seismic moment release to volume change scaling for volcanoes: A comparison with injection-induced seismicity. *Geophysical Research Letters*, 49, e2022GL099369. <https://doi.org/10.1029/2022GL099369>

Received 13 MAY 2022

Accepted 18 OCT 2022

### Author Contributions:

**Conceptualization:** Tom Kettlety, J. Michael Kendall

**Data curation:** Tom Kettlety, Diana C. Roman

**Formal analysis:** Tom Kettlety

**Funding acquisition:** J. Michael Kendall

**Investigation:** Tom Kettlety, J. Michael Kendall

**Methodology:** Tom Kettlety, J. Michael Kendall, Diana C. Roman

**Resources:** Tom Kettlety, Diana C. Roman

**Software:** Tom Kettlety

**Supervision:** J. Michael Kendall, Diana C. Roman

**Visualization:** Tom Kettlety

© 2022. The Authors.

This is an open access article under the terms of the [Creative Commons Attribution License](https://creativecommons.org/licenses/by/4.0/), which permits use, distribution and reproduction in any medium, provided the original work is properly cited.

## Self-Similarity of Seismic Moment Release to Volume Change Scaling for Volcanoes: A Comparison With Injection-Induced Seismicity

Tom Kettlety<sup>1</sup> , J. Michael Kendall<sup>1</sup> , and Diana C. Roman<sup>2</sup> 

<sup>1</sup>Department of Earth Sciences, University of Oxford, Oxford, UK, <sup>2</sup>Earth and Planets Laboratory, Carnegie Institution for Science, Washington, DC, USA

**Abstract** Estimates of intruded magma volume are critical for forecasting volcanic unrest. Geodetic modeling can provide such estimates but is of limited use in submarine and highly vegetated settings. A complementary approach could be to use estimates of seismic moment release. In this study, we examine the moment-volume scaling of several proximal volcanic earthquake sequences and compare it to that of injection-induced seismicity. We find a notable similarity in scaling between the volcanic sequences, which contrasts with the broad range of responses exhibited by anthropogenic injection-induced sequences. This may imply an underlying similarity in the geologic conditions for volcanoes that is distinct from induced seismicity settings. It could also allow for estimates of intruded volume to be made without geodetic information. This provides further insight into the factors controlling seismogenesis in these different settings and has implications for volcano seismology and injection-induced seismicity hazard estimation.

**Plain Language Summary** Knowing how much magma is beneath a volcano before or during an eruption can help forecast its behavior and aid evacuation or relief efforts. Currently, satellite images or sensitive measurements of the ground inflation are used to model the amount of magma, but this isn't always possible if the volcano is underwater or shrouded by tree cover. A proposed alternative to this is to use the size and number of earthquakes as a gauge on the amount of volume change occurring underground. The relationship between the total amount of energy released by earthquakes and volume change has been a key research area of earthquakes triggered in the injection of fluids by industries like geothermal energy or hydraulic fracturing (i.e., fracking). We study several well-recorded volcanoes and see that there is a similarity in the observed volume change and the amount of energy released from associated earthquakes. This is very different from the many examples of anthropogenic injection-induced seismicity, which show a very broad spread. This implies that the similar conditions under volcanoes lead to similar responses to volume changes. This helps us better understand and thus potentially mitigate the hazards of both volcanoes and industrial fluid injection.

## 1. Introduction

The analysis of volcanic seismicity is a key tool for eruption forecasting (Cameron et al., 2018). However, although well-monitored volcanoes show changes in seismic activity before eruptions, in practice these changes are generally only useful for forecasting eruption likelihood (and perhaps eruption timing). Thus, new insights into how precursory seismicity indicates other critical aspects of a complete forecast, including eruption volume, remain a grand challenge in volcanology (NASEM, 2017). Several recent studies have attempted to link the cumulative seismic moment of volcano-tectonic (VT) seismic sequences (Roman & Cashman, 2006) to intruded magma volume based on long-standing work focused on fluid injection volumes and anthropogenic injection-induced seismicity (e.g., McGarr, 1976). White and McCausland (2016) posited a link between the cumulative magnitude of so-called “distal VT seismicity” and intruded magma volumes.

In a re-examination of this proposed link using higher-quality data sets, Meyer et al. (2021) argued that cumulative seismic moment in VT sequences underpredicts intruded volume, especially for low-cumulative-moment VT sequences. However, Meyer et al. (2021) did not discriminate between proximal and distal VT seismicity, and both studies assumed equivalence between commonly reported local magnitudes ( $M_L$ ) and moment-magnitude ( $M_W$ ). We hypothesize that, due to spatial proximity of proximal VT seismicity to the intruded volume, and the greater accuracy in general of magnitude catalogs of proximally recorded earthquakes, proximal VT seismicity

**Writing – original draft:** Tom Kettlety, Diana C. Roman

**Writing – review & editing:** Tom Kettlety, J. Michael Kendall, Diana C. Roman

should better reflect intrusion volume. We test this hypothesis by accounting for magnitudes of proximal VT earthquakes in recent and well-characterized sequences with geodetically constrained intrusion volumes.

McGarr (1976) first hypothesized that there is a scaling between a volume change in the subsurface and the maximum seismic moment release. The recent increase in the rate of induced seismicity led McGarr (2014) to reformulate the relation as:

$$\Sigma M_o = 2G\Delta V \quad (1)$$

with total seismic moment  $M_o$ , shear modulus  $G$ , and volume change  $\Delta V$ . Whilst some case studies (e.g., Atkinson et al., 2016; Kim et al., 2018), have exceeded this hypothetical maximum, most induced seismicity cases are consistent with the reformulated McGarr relationship (e.g., Galis et al., 2017). Hereafter we will refer to anthropogenically triggered seismicity, stimulated by the injection of fluids during industrial processes, as “injection-induced” or simply “induced.”

In induced seismicity hazard assessments, the earthquake response of a reservoir is naturally of utmost importance. The measure of scaling between the seismic response and injected volume has been primarily quantified in two ways. Shapiro et al. (2010) developed the “seismogenic index,”  $S_I$ , which relates the number of events  $N$  above a given magnitude  $M$  to the volume injected  $\Delta V$ , using the Gutenberg-Richter  $b$ -value of the frequency-magnitude distribution:

$$S_I = \log_{10} \left( \frac{N(M)}{\Delta V} \right) + bM \quad (2)$$

This has been used in the development of volume scaling relationships for injection-induced seismicity (van der Elst et al., 2016), and in the real time forecasting of induced seismicity (as in Clarke et al. (2019) and Kettlety et al. (2021)).

Another measure has also been used, termed the “seismic efficiency,”  $S_{\text{eff}}$ . Hallo et al. (2014) introduced the parameter as an alteration to the McGarr (2014) relation, as a means of accounting for aseismic moment release. This takes the form:

$$\Sigma M_o = S_{\text{eff}} G \Delta V \quad (3)$$

and thus,  $S_{\text{eff}}$  is, more simply, the ratio of the total observed seismic moment release  $M_o$  to the hypothetical maximum,  $\sim G\Delta V$ , of McGarr (1976, 2014). It should be noted this “seismic efficiency” is not referring to the term used to describe the ratio of radiated to released energy, and in the following will only be used in the manner shown in Equation 3.

In published examples of injection-induced sequences, these parameters can vary over many orders of magnitude:  $-9 < S_I < 1$  (e.g., Dinske & Shapiro, 2013; van der Elst et al., 2016);  $-6 < \log_{10}(S_{\text{eff}}) < 3$  (e.g., Hallo et al., 2014; Maxwell, 2013; Verdon & Budge, 2018; Woo et al., 2019). Although typically  $S_{\text{eff}} < 1$ , it should be noted that the release of pre-existing tectonic strain energy during fault activation by injection could result in  $M_o$  being larger than  $2G\Delta V$  (the McGarr “limit”), as is evidenced, for example, by the 2017 Pohang seismicity (Kim et al., 2018).

Both  $S_{\text{eff}}$  and  $S_I$  encompass the structural, tectonic, lithological, and petrophysical conditions in the reservoir, convolving them together into a measure of how “seismogenic” the injection or intrusion is. They do not, however, allow one to state which of these controls is dominant, with further characterization of the seismicity and reservoir being required to do so. The broad range of both  $S_{\text{eff}}$  and  $S_I$  for induced sequences is reflective of the range of responses to injection of reservoirs. Several geologic factors could lead to this disparity, for example, the in situ stress anisotropy (e.g., Clarke et al., 2019; Kettlety et al., 2021; Lund Snee & Zoback, 2018); over- or under-pressure in the reservoir (Eaton & Schultz, 2018; Schultz et al., 2018); the prevalence of nearby faults (e.g., Schoenball et al., 2018); the alignment of faults relative to present day stresses or fractures (e.g., Kettlety & Verdon, 2021; Kettlety et al., 2020; Walsh & Zoback, 2015); or the friction behavior of the rocks (e.g., Faulkner et al., 2010; Zielke et al., 2017). It follows that regions with relatively similar geologic and tectonic conditions would be thought to exhibit broadly similar  $S_{\text{eff}}$  or  $S_I$ .

### 1.1. Structure of This Study

Following the works of White and McCausland (2016) and Meyer et al. (2021), we examine the scaling between seismic moment and volume change for several VT sequences, comparing them against many injection-induced examples. In this work, we take a rigorous approach to seismic magnitudes, accounting for the above complexities, and use relatively well-constrained examples of VT sequences, isolating events that are strictly associated with the inferred volume changes. We also take a much larger collection of injection-induced sequences, representative of the large observed variability, and compare those to the moment-volume scaling of the VT sequences. We then discuss the similarity in behavior (or lack thereof) and discuss its relevance to volcanic hazard assessment, the geologic controls on fluid-induced seismicity, and implications this may have for estimating volume changes in the crust using seismicity data.

## 2. Data and Methods

We have collected published examples of both volcanic and induced seismicity. Many are also used in Meyer et al. (2021), however we use a subset of high quality measurements of VT sequences, and a much larger collection of injection-induced examples. These are shown in the Table S1 in Supporting Information S1 for the 18 partial or complete volcanic sequences, and Table S2 in Supporting Information S1 for the 171 induced sequences.

### 2.1. Seismicity Selection

Care must be taken to correctly attribute seismic events in VT catalogs to the deformation signatures from which intruded volumes are modeled. Generally, one can retrieve seismicity catalogs during an intrusion episode for a volcano that also cover a large area around a volcanic edifice or span an entire volcanically active region. Most of the VT sequences analyzed in this study are examples of this, though the Bárðarbunga dyke intrusion demonstrates a particularly well-resolved case.

Whilst several deformation signatures are simultaneously occurring during the Askja-Bárðarbunga volcanism in 2014, the volume of the dyke growth is well constrained by geodetic and InSAR data (Sigmundsson et al., 2015) and seismicity was recorded throughout. Thus, it is a good target for study into the scaling between the moment and volume scaling. The available seismicity data (Ágústsdóttir et al., 2016; Green et al., 2015; Greenfield et al., 2020; Gudmundsson et al., 2016; Sigmundsson et al., 2015) contains many events which are not directly associated with the dyke intrusion alone but are VT events under and surrounding Bárðarbunga and Askja. Statements on total seismic moment release in the original publications include all these events, the largest of which are located under Bárðarbunga and associated with the caldera collapse (Gudmundsson et al., 2016). Thus, it is necessary to isolate the events strictly associated with the dyke growth (i.e., Figure 3 of Sigmundsson et al., 2015; Figure 2 of Gudmundsson et al., 2016). We take the seismicity catalogs themselves, and then calculate total seismic moment release and its associated uncertainty using the method below, rather than using the total seismic moment releases for the catalogs that are quoted in the original publications (e.g., Gudmundsson et al., 2016). Figure S1 in Supporting Information S1 shows the selection of the seismicity associated purely with the Bárðarbunga dyke intrusion from the surrounding VT events.

We isolate the events that are strictly associated with the deformation volume reported to get the most proximal seismicity. We take only events that occur adjacent to or within the deformation signatures and inferred sources of volume change, and only those that occur after the time the deformation started. This is what we term the “proximal” seismicity. We acknowledge that this is a functional definition rather than a more formal, procedural one. The proximal seismicity that took place after the volume change ceases is included in our moment release total, as it could still be the result of, and thus associated with, the deformation source. The exact spatiotemporal filters used in each of the VT case studies is given the supplementary materials (Text S3 in Supporting Information S1).

This should provide a greater control over the attributable seismicity (i.e., moment release) for a given volume change. In the Bárðarbunga case shown Figure S1 in Supporting Information S1, this means we do not include the diffuse clusters of seismicity to the northwest and southeast of the dyke, which is mostly seismicity that was associated with the caldera collapse and eruption of the nearby volcanoes. Though there is the possibility that some distal seismicity was triggered by longer length scale changes during the intrusion, they could be just associated with the other volcanic activity or other stress changes in the vicinity. Thus, we limit the scope of

seismicity to that which is undoubtedly attributable to the intrusion. The Bárðarbunga seismicity catalog, with its high-resolution, clustered event locations, enables this more detailed selection process.

Other VT sequences used in this work have more diffusive ellipsoidal clusters of seismicity. Precise event selection is naturally more limited for these cases, but we still include only events which are temporally and spatially associated with the deformation signatures used to invert for the volume changes. This generally means using only events directly beneath the edifice. Plots like Figure S1 in Supporting Information S1 for each of the VT sequences are also shown in the supplementary materials (Figures S2–S5 in Supporting Information S1).

## 2.2. Event Magnitudes and Total Seismic Moment

We use an informed series of approximations to estimate the total seismic moment, and its uncertainty, during each of the reported volcanic sequences from the seismicity catalogs. As discussed in an introduction to earthquake magnitudes in Text S1 in Supporting Information S1, catalogs rarely report moment magnitude. Uncertainties on the magnitude estimates are also very rarely given. Thus, we have developed a reasonable method to approximate the total seismic moment and estimate its uncertainty, which is detailed in Text S2 in Supporting Information S1.

Instead of accepting the simplification that local magnitude  $M_L$  can be assumed to equal moment magnitude  $M_w$ , we introduce a general  $M_w$ – $M_L$  relationship for small ( $M_L < 3$ ) event:  $M_w = 2/3 M_L + 1$ . This applies to all events with  $M_L < 3$ . This attempts to account for the widely observed (e.g., Butcher et al., 2020; Goertz-Allmann et al., 2011; Munafo et al., 2016) breakdown between  $M_w$  and  $M_L$  for small magnitude events. Deichmann (2017) showed this is due to the dispersive behavior of an attenuating medium and the scaling of amplitude and duration of the moment-rate function versus seismic moment. This is combined with a bias introduced by the form of the Wood-Anderson filter that is applied when calculating  $M_L$ . Whilst the exact form of the  $M_w$ – $M_L$  relationship used in this study is a generalization—ignoring the variations introduced by varying seismic instruments and network configurations (see Shelly et al., 2022)—it is still more robust than ignoring the  $M_w$ – $M_L$  discrepancy entirely. The slope value used here (2/3) is that which is theoretically expected (Deichmann, 2017). The remaining constant can be shown through simple algebra to set the magnitude where  $M_w$  and  $M_L$  become equal. Using this intercept value of 1 sets this “cross-over” magnitude at  $M 3$ , which is the magnitude below which this phenomenon is routinely observed to occur (e.g., Ross et al., 2016).

For injection-induced sequences, we use published values of total seismic moment from Dinske and Shapiro (2013), Maxwell (2013), Hallo et al. (2014), McGarr (2014), Buijze et al. (2015), Atkinson et al. (2016), McGarr and Barbour (2018), Clarke et al. (2019), Woo et al. (2019), and Kettlety et al. (2021).

## 2.3. Injected or Intruded Volume

We take the same approach as Meyer et al. (2021) and take published values of intruded volume from their original publications. These are given in Table S1 in Supporting Information S1. The volume changes are primarily compiled in Ebmeier et al. (2018), however, some recent and well constrained VT sequences are also included. Some sequences, such as the 2014 Bárðarbunga sequence, have been considered in total but also subdivided, as the intrusion was composed of several periods of activity, each with an estimate of the intruded volume. This allows us to construct a more detailed assessment of the scaling between volume change and moment release during each period of the sequence. Naturally, the volume and total seismic moment for each period build cumulatively.

The uncertainty in intruded volume is either taken directly from the original references themselves or is inferred from the ranges of values given from the modeled value (as in Meyer et al. (2021)). The fact that some estimates are given within a range is reflective of the uncertainty inherent in modeling deformation signals with simple models, such as Mogi (1958), Okada (1985), or Yang et al. (1988) sources. In these cases, we use the midpoint of the range as the  $\Delta V$  value, and  $\Delta V$  uncertainty is the extent of the range of the modeled volume changes. This is most likely an underestimation of the true error, and naturally does not account for the fact that Mogi, Okada, or Yang sources are simplifying spatially complex regions of deformation.

Injected volumes for injection-induced sequences are collected from the same sources as for the total seismic moment in the above. As injection data are collected to a high degree of precision ( $\sigma\Delta V < 1 \text{ m}^3$ ), the error in  $\Delta V$

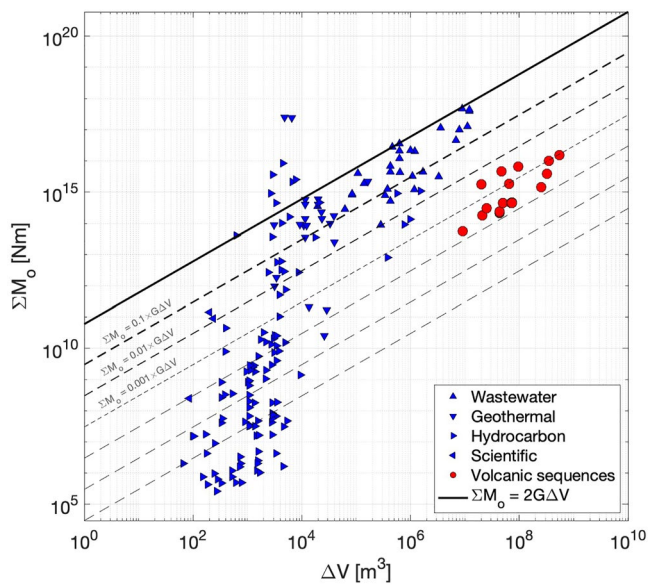


**Figure 1.** The relationship between total seismic moment ( $\Sigma M_0$ ) release and volume change ( $\Delta V$ ) for injection-induced seismicity (blue triangles), and volcanic sequences (red circles). The hypothetical maximum moment release given by the McGarr (2014) relation is shown as a solid black line, with shear modulus  $G = 30$  GPa. The dashed lines show the McGarr relationship modified by a seismic efficiency ( $S_{\text{eff}}$ ) term, after Hallo et al. (2014), to account for aseismic moment release. Each line represents an order of magnitude decrease in the scaling between  $\Sigma M_0$  and  $\Delta V$ , that is,  $S_{\text{eff}} = 0.1, 0.01, 0.001$ , etc.

for the injection sequence is assumed to be negligible. The compiled table of the 171 reported injection induced sequences is given in the supplementary materials (Table S2 in Supporting Information S1). The types of injection activity are given in Table S2 in Supporting Information S1 and are also shown in Figure 1.

#### 2.4. Seismic Efficiency and Seismogenic Index

To calculate the seismic efficiency  $S_{\text{eff}}$  and seismogenic index  $S_I$  for each VT data set, we use Equations 2 and 3, the calculated  $\Sigma M_0$ , and the published  $\Delta V$ . Uncertainty in both parameters is propagated through, using the standard formulations. A Gutenberg-Richter  $b$ -value is calculated using the maximum likelihood approach of Aki (1965), with updated uncertainty estimates of Tinti and Mulargia (1987) (see Marzocchi & Sandri, 2003). We find the magnitude of completeness  $M_{\text{min}}$  using the  $b$ -value stability method of Cao and Gao (2002), following the procedure of Roberts et al. (2015). This gives a  $b$ -value, its uncertainty  $\sigma_b$ , and  $M_{\text{min}}$ , which are all used in the calculation of  $S_I$  and its uncertainty.

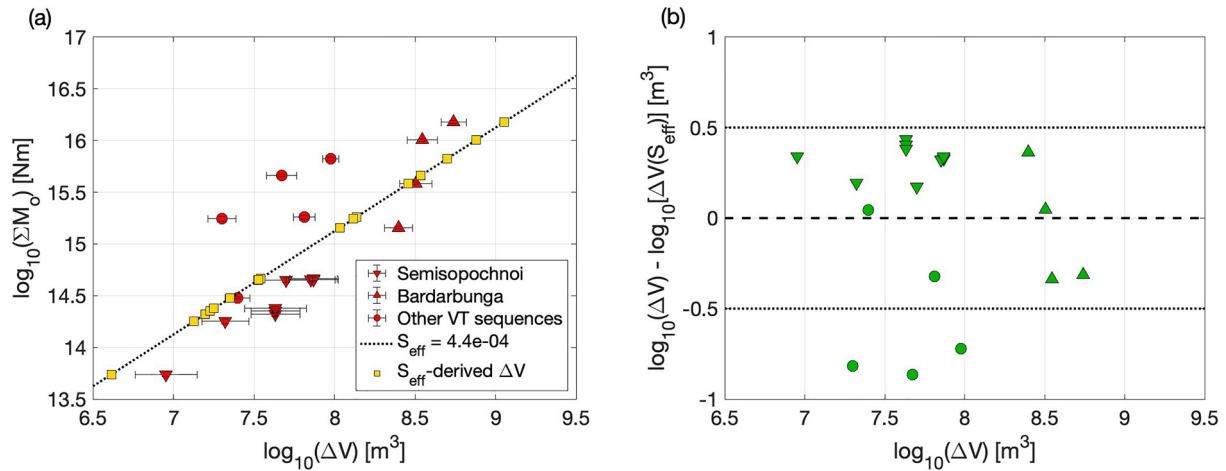
### 3. Results

Figure 1 shows the compiled total seismic moment release values and intruded or injected volumes, comparing the injection-induced sequences and the VT sequences. The results for the volcanic sequences are also detailed in Table S1 in Supporting Information S1. We observe a clear distinction between the range of seismic efficiencies exhibited between the two populations. Induced sequences show a very broad range (particularly for volume changes of  $\sim 10^4$  m<sup>3</sup> or less), from  $S_{\text{eff}} > 1$  to  $\log_{10}(S_{\text{eff}}) < -6$ . In contrast, the VT sequences fall in a notably narrower range of  $-4 < \log_{10}(S_{\text{eff}}) < -2$ . These VT sequences also broadly follow the linear trend expected from the McGarr (2014) relationship.

This clustering of volcanic sequences is noteworthy as it suggests a similarity in the physical processes underlying the activation of faults (e.g., stress conditions, rock types, frictional behavior, etc.) in volcanic sequences that is dissimilar to injection-induced sequences. Geologic factors like these have been shown to control the dynamics of seismicity in volcanic intrusions, such as stress conditions and rock friction in the modeling study of Heimisson and Segall (2020), or stressing rate in Pedersen et al. (2007).

With Pohang (Kim et al., 2018) and several hydraulic fracturing examples from the Western Canadian Sedimentary Basin (Atkinson et al., 2016) cases being clear exceptions, most of the largest induced cases appear to conform to the hypothetical maximum moment release of the McGarr (2014). The volcanic sequences also conform to the trend of McGarr (2014)—that is, more volume change leads to more seismic moment release—except with a seismic moment release around four orders of magnitude lower. As discussed above, this offset can be attributed to the geologic conditions increasing the proportion of aseismic deformation, systematically lowering  $S_{\text{eff}}$  for volcanic systems relative to the largest induced seismicity cases. Whilst the shear modulus  $G$  is a parameter in the McGarr relationship, and could be systematically lower in volcanic settings, the four orders of magnitude difference naturally cannot purely be the result of a reduction in  $G$ . It is more likely that a greater proportion of aseismic moment release is occurring in volcanic settings when compared to the induced settings that were used to evidence the McGarr “limit.”

Figure 2 examines the VT sequences in closer detail, comparing the volume estimated using a fitted, constant  $S_{\text{eff}}$ , assuming a linear relationship between  $\Sigma M_0$  and  $\Delta V$ . We note that the residual between the geodetically derived- $\Delta V$  and the constant  $S_{\text{eff}}$ -derived  $\Delta V$  is less than half an order of magnitude, similar in scale to the uncertainty assumed in Meyer et al. (2021), and most likely less than that which could be expected when inverting volume change based on a simplified source.



**Figure 2.** (a) The  $\Sigma M_0 - \Delta V$  relationship for the studied volcanic sequences. A  $S_{\text{eff}}$  is calculated through a least-squares inversion of the data, using Equation 3, with  $G = 30$  GPa. Red triangles and circles show the published data, whilst yellow squares show the  $\Delta V$  if the fitted  $S_{\text{eff}}$  is used to calculate a value from the measured total seismic moment release. Semisopchnoi and Bárðarbunga have been plotted as triangles, as many data points shown here are different phases of their respective intrusions. (b) The residual  $\log_{10}(\Delta V)$  between the published  $\Delta V$  values and that found when a constant  $S_{\text{eff}}$  is assumed. For most VT sequences, the difference would be less than  $\pm 0.5$  orders of magnitude.

## 4. Discussion

### 4.1. Lower $\Delta V$ Scatter and Selection Effects

There does appear to be a discontinuity in the  $\Sigma M_0 - \Delta V$  behavior around  $10^4 \text{ m}^3$ , with induced sequences above this volume broadly exhibiting a similar, larger  $S_{\text{eff}}$ , and the variability in  $S_{\text{eff}}$  increasing markedly below this  $\Delta V$ . It is challenging to assess the underlying cause for this behavior.

Likely factors affecting the patterns seen in the injection-induced sequences will be band-limited recordings and reporting biases. For the former, downhole observations of induced seismicity, most commonly made during hydraulic fracturing operations, may underestimate seismic moment systematically due to the short period instruments used. As moment magnitude is calculated using the magnitude of the low frequency plateau of the amplitude spectrum (e.g., see Butcher et al., 2020), and short period instruments are less sensitive to lower frequencies, this can lead to biases. However, these effects are generally underestimate magnitude by less than a magnitude unit (Kettlety et al., 2021; Stork et al., 2014), and so would not account for the entirety of the scatter seen at  $\Delta V < 10^4 \text{ m}^3$ .

As for reporting biases, the cases causing the largest seismicity are more widely studied and published, giving the appearance of more high-volume, high-moment release sequences. The data from these more seismically active cases are more widely available as the events will be recorded by regional networks operated by agencies which release data publicly. McGarr (2014) compiled many of these cases to base arguments concerning the hypothetical maximum possible moment release.

The seismicity data acquired during targeted, local monitoring of injection operations required to detect lower magnitude ( $M < 1$ ) seismicity are generally proprietary, as is its accompanying injected data, and so only a small subset of operations are ever published or compiled (such as in Maxwell, 2013). For example, there are unconventional hydrocarbon fields, such as parts of the Western Canadian Sedimentary Basin, which are relatively seismically quiescent, with only  $\sim 1\%$  of wells being associated with significant ( $M > 3$ ) seismicity (Atkinson et al., 2016). This is despite the presence of a very large hydraulic fracturing and wastewater disposal industry, with volumes per pad far greater than  $10^4 \text{ m}^3$ . This large number of “quiet” operations do not produce widely felt ( $M > 3$ ) seismicity, and thus are not detected by regional networks, and not represented in the literature. Some studies (e.g., Skoumal et al., 2020) have linked field-scale injection to regional seismicity in a more distributed fashion, where it is unfeasible to directly attribute specific operations (i.e., a specific  $\Delta V$ ) to some resulting seismicity (i.e., a single  $\Sigma M_0$ ). Our study compiles the available, published examples, and naturally would be improved by more extensive reporting of seismic and operational data. With many high volume wells not

stimulating regionally detectable events, it is likely that adding more higher  $\Delta V$  induced sequences would simply fill out the broad range of  $S_{\text{eff}}$  exhibited at  $\Delta V < 10^4 \text{ m}^3$  to higher volumes of injection.

Selection bias effects are also naturally present in the studied VT sequences. For example, the 2008 eruption of Okmok in the Alaskan Aleutian Islands displays a markedly different behavior to the sequences shown in Figure 1. A long-term-inter-eruptive inflationary period was generally aseismic (Larsen et al., 2015; Lu et al., 2010), however, this period immediately followed a previous eruption in 2007, and thus the overall connection between an episode of intrusion and the resulting seismicity are quite different. This makes it less comparable to the cases of proximal VT seismicity studied here, where there is an intrusion or deformation signal associated with proximal seismicity. During the pre-eruptive period of Hekla in 2000 (Hoskuldsson et al., 2007) there was a steady, low rate of inflation (Sturkell et al., 2006), however local seismic monitoring of the volcano was not sensitive to much of the activity during this time (Einarsson, 2018).

There are not many volcanic examples of a precursory deformation signal with a sufficiently dense, local seismic network, and this lack of monitoring is a limitation for this kind of analysis. Also, for volcanic sequences, there is a minimum observable (or more precisely modellable)  $\Delta V$ , in-part controlled by the minimum volume that can be routinely inverted from deformation signals measurable by InSAR or geodetic methods. However, this study attempts to just take the best possible data, carefully treat the event selection and magnitudes, and examine the trends therein. It should be noted that more evidence from high-quality seismicity and deformation data could change the interpretation and results we have found here.

#### 4.2. Data Aggregation and Treatment

In compiling the estimates of total seismic moment release and intruded volume, several assumptions must be made. We rely on the accuracy of the published model inversions for volume change, which assume simplified deformation sources. For the seismic catalogs, each uncertainty will act to affect the total  $M_0$ . These include using magnitude scales inappropriate for the region, only reporting  $M_L$ , poor location quality, and the common assumption that different magnitudes can be simply equated. These each act to highlight problems with data quality that are common across the seismological literature. This is particularly true for data associated with volcanoes, where the monitoring environment is incredibly challenging.

Calculating total  $M_0$  necessitates the use of  $M_w$ , and thus the conversion of reported magnitudes to this scale. The assumption of a single  $M_w$ - $M_L$  relationship for small events will impact the magnitude of the moment releases calculated here, but not significantly so. The error will be of a similar size (from 0.1 to 0.5 magnitude units), to the underlying magnitudes themselves (Shelly et al., 2022; Stork et al., 2014). The inappropriate inclusion of large events not directly associated with the volume change would impact the total  $M_0$  far more, increasing it by many orders of magnitude (as in the Bárðarbunga case described above). By examining each sequence in more detail, we have attempted to account for this inaccuracy. Even with these uncertainties in mind, these results still provide a promising means of understanding the seismic response to volume changes (Figure 2).

#### 5. Conclusions

In this study, we examine the scaling between total seismic moment release and volume change for several volcanic and many injection-induced earthquake sequences. We carefully select relevant VT seismicity from publicly available catalogs, and derive moment release from mostly local magnitude estimates, accounting for the divergence between that and moment magnitude. We then compare the moment-volume scaling behavior to many published injection-induced sequences and find that volcanic sequences have a significantly more similar relationship between moment release and volume change, and one that appears to mirror the McGarr (2014) relationship, albeit at a lower seismic efficiency. This is evidenced by a relatively small range of seismic efficiencies,  $S_{\text{eff}}$ , for the volcanic sequences:  $-4 < \log_{10}(S_{\text{eff}}) < -2$ , with an average  $S_{\text{eff}} \sim 5e-4$ .

This finding means an independent estimate of intruded volume could be made for volcanic sequences in regions with limited geodetic data. In such circumstances, where the inversion of volume changes at depth cannot be constrained by, for example, InSAR, measurements of seismicity could be used to make a preliminary volume estimate, using:  $\Delta V = \Sigma M_0 / (S_{\text{eff}} G)$ . Figure 2 supports that the uncertainty on such an estimate would not be unreasonably large—around half an order of magnitude.

Given the nature of  $S_{\text{eff}}$  and its encapsulation of an area's seismic response to volume changes, we posit that this result also implies that the volcanic settings compared here may have more similar “seismogenetic” conditions, than for the induced sequences. The broad range of geologic and tectonic conditions that are exhibited for induced sequences, which span relatively shallow sedimentary basins to deep geothermal operations in igneous provinces, may underpin this observation. The stark difference in the behavior of the moment-volume scaling we observe may confirm the finding that similar geologic conditions result in similar seismic responses, which has been difficult to constrain (e.g., Galis et al., 2017).

This study has several ramifications for our understanding of the geologic controls underlying induced seismicity, as well as a method of estimating intruded volumes. In combining data from the two settings, we can improve understanding of both injection-induced and volcano seismicity, and aid in hazard analysis through the quantification of volume change in areas where that may not have been possible. By examining the volcanic settings with similar controls on seismicity, this study can help in better understanding the likelihood of felt earthquakes for induced seismicity. This is particularly relevant to several industries—for example, hydraulic fracturing, wastewater disposal, geothermal energy, CO<sub>2</sub> storage—each of which plays a crucial role in the coming decades.

### Conflict of Interest

The authors declare no conflicts of interest relevant to this study.

### Data Availability Statement

All seismicity catalogs and volume changes were collected from the published sources referenced in the text (Ágústsdóttir et al., 2016; DeGrandpre et al., 2019; Fournier et al., 2010; Gudmundsson et al., 2016; Hickey et al., 2020; Meyer et al., 2021; Neal et al., 2019; Parks et al., 2015; Power & Lalla, 2010; Power et al., 2019; Roman et al., 2021; Sigmundsson et al., 2015) and are available online. Data underlying Figures 1 and 2 and are provided in Table S1 in Supporting Information S1 and Table S2 in Supporting Information S1 are available to download from the UK National Environmental Research Council's (NERC) National Geoscience Data Centre (NGDC), accessible here: <https://doi.org/10.5285/bf555da1-bf69-4389-947b-102adc74324f>.

### Acknowledgments

We would like to thank the editor Daoyuan Sun, and reviewers, Art McGarr and Freysteinn Sigmundsson, for their constructive feedback which improved the manuscript. This work was funded through UK National Environmental Research Council UKUH project (NERC, NE/R018006/1) and the ACT3 (EC Project 691712) SHARP-Storage project (project 327342).

### References

- Ágústsdóttir, T., Woods, J., Greenfield, T., Green, R. G., White, R. S., Winder, T., et al. (2016). Strike-slip faulting during the 2014 Bárðarbunga-Holuhraundike intrusion, central Iceland. *Geophysical Research Letters*, *43*(4), 1495–1503. <https://doi.org/10.1002/2015GL067423>
- Aki, K. (1965). Maximum likelihood estimate of  $b$  in the formula  $\log N = a - bM$  and its confidence. *Bulletin of Earthquake Research Institute of the University of Tokyo*, *43*, 237–239.
- Atkinson, G. M., Eaton, D. W., Ghofrani, H., Walker, D. M., Cheadle, B., Schultz, R. J., et al. (2016). Hydraulic fracturing and seismicity in the Western Canada Sedimentary Basin. *Seismological Research Letters*, *87*(3), 631–647. <https://doi.org/10.1785/0220150263>
- Buijze, L., Wassing, B., Fokker, P. A., & van Wees, J. D. (2015). Moment partitioning for injection-induced seismicity: Case studies & insights from numerical modeling. *Proceedings World Geothermal Congress*, 19–25.
- Butcher, A., Luckett, R., Kendall, J. M., & Baptie, B. (2020). Seismic magnitudes, corner frequencies, and microseismicity: Using ambient noise to correct for high-frequency attenuation. *Bulletin of the Seismological Society of America*, *110*(3), 1260–1275. <https://doi.org/10.1785/0120190032>
- Cameron, C. E., Prejean, S. G., Coombs, M. L., Wallace, K. L., Power, J. A., & Roman, D. C. (2018). Alaska Volcano observatory alert and forecasting timeliness: 1989–2017. *Frontiers of Earth Science*, *86*. <https://doi.org/10.3389/FEART.2018.00086/>
- Cao, A., & Gao, S. S. (2002). Temporal variation of seismic  $b$ -values beneath northeastern Japan island arc. *Geophysical Research Letters*, *29*(9), 481–483. <https://doi.org/10.1029/2001gl013775>
- Clarke, H., Verdon, J. P., Kettlely, T., Baird, A. F., & Kendall, J. M. (2019). Real-time imaging, forecasting, and management of human-induced seismicity at Preston new road, Lancashire, England. *Seismological Research Letters*, *90*(5), 1902–1915. <https://doi.org/10.1785/0220190110>
- DeGrandpre, K. G., Pesicek, J. D., Lu, Z., DeShon, H. R., & Roman, D. C. (2019). High rates of inflation during a noneruptive episode of seismic unrest at semisopchnoi Volcano, Alaska in 2014–2015. *Geochemistry, Geophysics, Geosystems*, *20*(12), 6163–6186. <https://doi.org/10.1029/2019GC008720>
- Deichmann, N. (2017). Theoretical basis for the observed break in  $M_L/M_w$  scaling between small and large earthquakes. *Bulletin of the Seismological Society of America*, *107*(2), 505–520. <https://doi.org/10.1785/0120160318>
- Dinske, C., & Shapiro, S. A. (2013). Seismotectonic state of reservoirs inferred from magnitude distributions of fluid-induced seismicity. *Journal of Seismology*, *17*(1), 13–25. <https://doi.org/10.1007/s10950-012-9292-9>
- Eaton, D. W., & Schultz, R. J. (2018). Increased likelihood of induced seismicity in highly overpressured shale formations. *Geophysical Journal International*, *214*(1), 751–757. <https://doi.org/10.1093/gji/ggy167>
- Ebmeier, S. K., Andrews, B. J., Araya, M. C., Arnold, D. W. D., Biggs, J., Cooper, C., et al. (2018). Synthesis of global satellite observations of magmatic and volcanic deformation: Implications for volcano monitoring & the lateral extent of magmatic domains. *Journal of Applied Volcanology*, *7*(1), 1–26. <https://doi.org/10.1186/s13617-018-0071-3>



- Einarsson, P. (2018). Short-term seismic precursors to Icelandic eruptions 1973–2014. *Frontiers of Earth Science*, 6, 45. <https://doi.org/10.3389/FEART.2018.00045>
- Faulkner, D. R., Jackson, C. A. L., Lunn, R. J., Schlische, R. W., Shipton, Z. K., Wibberley, C. A. J., & Withjack, M. O. (2010). A review of recent developments concerning the structure, mechanics and fluid flow properties of fault zones. *Journal of Structural Geology*, 32(11), 1557–1575. <https://doi.org/10.1016/j.jsg.2010.06.009>
- Fournier, T. J., Pritchard, M. E., & Riddick, S. N. (2010). Duration, magnitude, and frequency of subaerial volcano deformation events: New results from Latin America using InSAR and a global synthesis. *Geochemistry, Geophysics, Geosystems*, 11(1). <https://doi.org/10.1029/2009GC002558>
- Galis, M., Ampuero, J. P., Mai, P. M., & Cappa, F. (2017). Induced seismicity provides insight into why earthquake ruptures stop. *Science Advances*, 3(12), eaap7528. <https://doi.org/10.1126/sciadv.aap7528>
- Goertz-Allmann, B. P., Edwards, B., Bethmann, F., Deichmann, N., Clinton, J., Fäh, D., & Giardini, D. (2011). A new empirical magnitude scaling relation for Switzerland. *Bulletin of the Seismological Society of America*, 101(6), 3088–3095. <https://doi.org/10.1785/0120100291>
- Green, R. G., Greenfield, T., & White, R. S. (2015). Triggered earthquakes suppressed by an evolving stress shadow from a propagating dyke. *Nature Geoscience*, 8(8), 629–632. <https://doi.org/10.1038/ngeo2491>
- Greenfield, T., White, R. S., Winder, T., & Ágústadóttir, T. (2020). Seismicity of the Askja and Bárðarbunga volcanic systems of Iceland, 2009–2015. *Journal of Volcanology and Geothermal Research*, 391, 106432. <https://doi.org/10.1016/j.jvolgeores.2018.08.010>
- Gudmundsson, M. T., Jónsdóttir, K., Hooper, A., Holohan, E. P., Halldórsson, S. A., Ófeigsson, B. G., et al. (2016). Gradual caldera collapse at Bárðarbunga volcano, Iceland, regulated by lateral magma outflow. *Science*, 353(6296). <https://doi.org/10.1126/science.aaf8988>
- Hallo, M., Oprsál, I., Eisner, L., & Ali, M. Y. (2014). Prediction of magnitude of the largest potentially induced seismic event. *Journal of Seismology*, 18(3), 421–431. <https://doi.org/10.1007/s10950-014-9417-4>
- Heimisson, E. R., & Segall, P. (2020). Physically consistent modeling of dike-induced deformation and seismicity: Application to the 2014 Bárðarbunga dike, Iceland. *Journal of Geophysical Research: Solid Earth*, 125(2), e2019JB018141. <https://doi.org/10.1029/2019JB018141>
- Hickey, J., Lloyd, R., Biggs, J., Arnold, D., Mothes, P., & Muller, C. (2020). Rapid localized flank inflation and implications for potential slope instability at Tungurahua volcano, Ecuador. *Earth and Planetary Science Letters*, 534, 116104. <https://doi.org/10.1016/j.epsl.2020.116104>
- Höskuldsson, Á., Óskarsson, N., Pedersen, R., Grönvold, K., Vogfjörð, K., & Ólafsdóttir, R. (2007). The millennium eruption of Hekla in February 2000. *Bulletin of Volcanology*, 70(2), 169–182. <https://doi.org/10.1007/S00445-007-0128-3>
- Kettlety, T., & Verdon, J. P. (2021). Fault triggering mechanisms for hydraulic fracturing-induced seismicity from the Preston new road, UK case study. *Frontiers of Earth Science*, 9, 670771. <https://doi.org/10.3389/feart.2021.670771>
- Kettlety, T., Verdon, J. P., Butcher, A., Hampson, M., & Craddock, L. (2021). High-resolution imaging of the ML 2.9 August 2019 earthquake in Lancashire, United Kingdom, induced by hydraulic fracturing during Preston new road PNR-2 operations. *Seismological Research Letters*, 92(1), 151–169. <https://doi.org/10.1785/0220200187>
- Kettlety, T., Verdon, J. P., Werner, M. J., & Kendall, J. M. (2020). Stress transfer from opening hydraulic fractures controls the distribution of induced seismicity. *Journal of Geophysical Research: Solid Earth*, 125(1), e2019JB018794. <https://doi.org/10.1029/2019JB018794>
- Kim, K.-H., Ree, J.-H., Kim, Y.-H., Kim, S., Kang, S. Y., & Seo, W. (2018). Assessing whether the 2017 Mw 5.4 Pohang earthquake in South Korea was an induced event. *Science*, 360(6392), 1007–1009. <https://doi.org/10.1126/science.aat6081>
- Larsen, J., Neal, C. A., Schaefer, J. R., Kaufman, M., & Lu, Z. (2015). The 2008 phreatomagmatic eruption of Okmok volcano, Aleutian Islands, Alaska: Chronology, deposits, and landform changes. In *Alaska division of geological & geophysical surveys report of investigation*. <https://doi.org/10.14509/29405>
- Lu, Z., Dzurisin, D., Biggs, J., Wicks, C., & McNutt, S. (2010). Ground surface deformation patterns, magma supply, and magma storage at Okmok volcano, Alaska, from InSAR analysis: 1. Interruption deformation, 1997–2008. *Journal of Geophysical Research*, 115(B5), 0–02. <https://doi.org/10.1029/2009JB006969>
- Lund Snee, J.-E., & Zoback, M. D. (2018). State of stress in Texas: Implications for induced seismicity. *The Leading Edge*, 37(2), 127–134. <https://doi.org/10.1002/2016GL070974>
- Marzocchi, W., & Sandri, L. (2003). A review and new insights on the estimation of the b-value and its uncertainty. *Annals of Geophysics*, 46(6), 1271–1282. <https://doi.org/10.4401/ag-3472>
- Maxwell, S. (2013). Unintentional seismicity induced by hydraulic fracturing. *CSEG Recorder*, 38.
- McGarr, A. F. (1976). Seismic moments and volume changes. *Journal of Geophysical Research*, 81(8), 1487–1494. <https://doi.org/10.1029/jb081i008p01487>
- McGarr, A. F. (2014). Maximum magnitude earthquakes induced by fluid injection. *Journal of Geophysical Research: Solid Earth*, 119(2), 1008–1019. <https://doi.org/10.1002/2013JB010597>
- McGarr, A. F., & Barbour, A. J. (2018). Injection-induced moment release can also be aseismic. *Geophysical Research Letters*, 45(11), 5344–5351. <https://doi.org/10.1029/2018GL078422>
- Meyer, K., Biggs, J., & Aspinall, W. (2021). A Bayesian reassessment of the relationship between seismic moment and magmatic intrusion volume during volcanic unrest. *Journal of Volcanology and Geothermal Research*, 419, 107375. <https://doi.org/10.1016/j.jvolgeores.2021.107375>
- Mogi, K. (1958). Relations between the eruptions of various volcanoes and the deformations of the ground surfaces around them. *Bulletin of the Earthquake Research Institute, University of Tokyo*, 36, 99–134.
- Munafò, I., Malagnini, L., & Chiaraluca, L. (2016). On the relationship between  $M_w$  and  $M_L$  for small earthquakes. *Bulletin of the Seismological Society of America*, 106(5), 2402–2408. <https://doi.org/10.1785/0120160130>
- National Academies of Sciences, Engineering, and Medicine. (2017). *Volcanic eruptions and their repose, unrest, precursors, and timing*. The National Academies Press. <https://doi.org/10.17226/24650>
- Neal, C. A., Brantley, S. R., Antolik, L., Babb, J. L., Burgess, M., Calles, K., et al. (2019). The 2018 rift eruption and summit collapse of Kīlauea Volcano. *Science*, 363, 367–374. <https://doi.org/10.1126/science.aav7046>
- Okada, Y. (1985). Surface deformation due to shear and tensile faults in a half-space. *Bulletin of the Seismological Society of America*, 75(4), 1135–1154. <https://doi.org/10.1785/BSSA0750041135>
- Parks, M. M., Moore, J. D. P., Papanikolaou, X., Biggs, J., Mather, T. A., Pyle, D. M., et al. (2015). From quiescence to unrest: 20 years of satellite geodetic measurements at Santorini volcano, Greece. *Journal of Geophysical Research: Solid Earth*, 120(2), 1309–1328. <https://doi.org/10.1002/2014JB011540>
- Pedersen, R., Sigmundsson, F., & Einarsson, P. (2007). Controlling factors on earthquake swarms associated with magmatic intrusions: Constraints from Iceland. *Journal of Volcanology and Geothermal Research*, 162(1–2), 73–80. <https://doi.org/10.1016/J.JVOLGEORES.2006.12.010>
- Power, J. A., Friberg, P. A., Haney, M. M., Parker, T., Stihler, S. D., & Dixon, J. P. (2019). A unified catalog of earthquake hypocenters and magnitudes at Volcanoes in Alaska — 1989 to 2018. <https://doi.org/10.3133/sir20195037>

- Power, J. A., & Lalla, D. J. (2010). Seismic observations of Augustine Volcano, 1970–2007, chapter 1 of power. In J. A. Coombs, M. L. Coombs, & J. T. Freymueller (Eds.), *The 2006 eruption of Augustine Volcano, Alaska: U.S. Geological survey professional paper 1769* (pp. 3–40). Retrieved from [https://pubs.usgs.gov/pp/1769/chapters/p1769\\_chapter01.pdf](https://pubs.usgs.gov/pp/1769/chapters/p1769_chapter01.pdf)
- Roberts, N. S., Bell, A. F., & Main, I. G. (2015). Are volcanic seismic b-values high, and if so when? *Journal of Volcanology and Geothermal Research*, 308, 127–141. <https://doi.org/10.1016/j.jvolgeores.2015.10.021>
- Roman, D. C., & Cashman, K. V. (2006). The origin of volcano-tectonic earthquake swarms. *Geology*, 34(6), 457–460. <https://doi.org/10.1130/G22269.1>
- Roman, D. C., Soldati, A., Dingwell, D. B., Houghton, B. F., & Shiro, B. R. (2021). Earthquakes indicated magma viscosity during Kīlauea's 2018 eruption. *Nature*, 592(7853), 237–241. <https://doi.org/10.1038/s41586-021-03400-x>
- Ross, Z. E., Ben-Zion, Y., White, M. C., & Vernon, F. L. (2016). Analysis of earthquake body wave spectra for potency and magnitude values: Implications for magnitude scaling relations. *Geophysical Journal International*, 207(2), 1158–1164. <https://doi.org/10.1093/GJI/GGW327>
- Schoenball, M., Walsh, F. R., Weingarten, M. B., & Ellsworth, W. L. (2018). How faults wake up: The Guthrie-Langston, Oklahoma earthquakes. *The Leading Edge*, 37(2), 100–106. <https://doi.org/10.1190/le37020100.1>
- Schultz, R. J., Atkinson, G. M., Eaton, D. W., Gu, Y. J., & Kao, H. (2018). Hydraulic fracturing volume is associated with induced earthquake productivity in the Duvernay play. *Science*, 359(6373), 304–308. <https://doi.org/10.1126/science.aao0159>
- Shapiro, S. A., Dinske, C., Langenbruch, C., & Wenzel, F. (2010). Seismogenic index and magnitude probability of earthquakes induced during reservoir fluid stimulations. *The Leading Edge*, 29(3), 304–309. <https://doi.org/10.1190/1.11901.1.3353727>
- Shelly, D. R., Mayeda, K., Barno, J., Whidden, K. M., Moschetti, M. P., Llenos, A. L., et al. (2022). A big problem for small earthquakes: Benchmarking routine magnitudes and conversion relationships with coda envelope-derived Mw in southern Kansas and northern Oklahoma. *Bulletin of the Seismological Society of America*, 112(1), 210–225. <https://doi.org/10.1785/0120210115>
- Sigmundsson, F., Hooper, A., Hreinsdóttir, S., Vogfjörð, K. S., Ófeigsson, B. G., Heimisson, E. R., et al. (2015). Segmented lateral dyke growth in a rifting event at Bárðarbunga volcanic system, Iceland. *Nature*, 517(7533), 191–195. <https://doi.org/10.1038/nature14111>
- Skoumal, R. J., Barbour, A. J., Brudzinski, M. R., Langenkamp, T., & Kaven, J. O. (2020). Induced seismicity in the Delaware Basin, Texas. *Journal of Geophysical Research: Solid Earth*, 125(1). <https://doi.org/10.1029/2019JB018558>
- Stork, A. L., Verdon, J. P., & Kendall, J. M. (2014). The robustness of seismic moment and magnitudes estimated using spectral analysis. *Geophysical Prospecting*, 62(4), 862–878. <https://doi.org/10.1111/1365-2478.12134>
- Sturkell, E., Einarsson, P., Sigmundsson, F., Geirsson, H., Ólafsson, H., Pedersen, R., et al. (2006). Volcano geodesy and magma dynamics in Iceland. *Journal of Volcanology and Geothermal Research*, 150(1–3), 14–34. <https://doi.org/10.1016/J.JVOLGEORES.2005.07.010>
- Tinti, S., & Mulargia, F. (1987). Confidence intervals of b values for grouped magnitudes. *Bulletin of the Seismological Society of America*, 77(6), 2125–2134. <http://www.bssaonline.org/content/77/6/2125.abstract>
- van der Elst, N. J., Page, M. T., Weiser, D. A., Goebel, T. H. W., & Hosseini, S. M. (2016). Induced earthquake magnitudes are as large as (statistically) expected. *Journal of Geophysical Research: Solid Earth*, 121(6), 4575–4590. <https://doi.org/10.1002/2016JB012818>
- Verdon, J. P., & Budge, J. (2018). Examining the capability of statistical models to mitigate induced seismicity during hydraulic fracturing of shale gas reservoirs. *Bulletin of the Seismological Society of America*, 108(2), 690–701. <https://doi.org/10.1785/0120170207>
- Walsh, F. R., & Zoback, M. D. (2015). Oklahoma's recent earthquakes and saltwater disposal. *Science Advances*, 1(e1500195), 1–9. <https://doi.org/10.1126/sciadv.1500195>
- White, R., & McCausland, W. (2016). Volcano-tectonic earthquakes: A new tool for estimating intrusive volumes and forecasting eruptions. *Journal of Volcanology and Geothermal Research*, 309, 139–155. <https://doi.org/10.1016/j.jvolgeores.2015.10.020>
- Woo, J.-U., Kim, M., Sheen, D.-H., Kang, T.-S., Rhie, J., Grigoli, F., et al. (2019). An in-depth seismological analysis revealing a causal link between the 2017 MW 5.5 Pohang earthquake and EGS project. *Journal of Geophysical Research: Solid Earth*, 124(12), 13060–13078. <https://doi.org/10.1029/2019JB018368>
- Yang, X.-M., Davis, P. M., & Dieterich, J. H. (1988). Deformation from inflation of a dipping finite prolate spheroid in an elastic half-space as a model for volcanic stressing. *Journal of Geophysical Research*, 93(B5), 4249–4257. <https://doi.org/10.1029/JB093IB05P04249>
- Zielke, O., Galis, M., & Mai, P. M. (2017). Fault roughness and strength heterogeneity control earthquake size and stress drop. *Geophysical Research Letters*, 44(2), 777–783. <https://doi.org/10.1002/2016GL071700>

## References From the Supporting Information

- Butcher, A., Luckett, R., Verdon, J. P., Kendall, J. M., Baptie, B., & Wookey, J. (2017). Local magnitude discrepancies for near-event receivers: Implications for the U.K. traffic-light scheme. *Bulletin of the Seismological Society of America*, 107(2), 532–541. <https://doi.org/10.1785/0120160225>
- Luckett, R., Ottemöller, L., Butcher, A., & Baptie, B. (2019). Extending local magnitude ML to short distances. *Geophysical Journal International*, 216(2), 1145–1156. <https://doi.org/10.1093/gji/ggy484>